Vol 18 No 1, January 2009
1674-1056/2009/18(01)/0303-06

Chinese Physics B

© 2009 Chin. Phys. Soc.
and IOP Publishing Ltd

A super junction SiGe low-loss fast switching power diode*

Ma Li(马 丽)[a)†] and Gao Yong(高 勇)[b)]

[a)] *Department of Applied Physics, Xi'an University of Technology, Xi'an* 710048, *China*

[b)] *Department of Electronics Engineering, Xi'an University of Technology, Xi'an* 710048, *China*

(Received 15 January 2008; revised manuscript received 22 June 2008)

This paper proposes a novel super junction (SJ) SiGe switching power diode which has a columnar structure of alternating p^- and n^- doped pillar substituting conventional n^- base region and has far thinner strained SiGe p^+ layer to overcome the drawbacks of existing Si switching power diode. The SJ SiGe diode can achieve low specific on-resistance, high breakdown voltages and fast switching speed. The results indicate that the forward voltage drop of SJ SiGe diode is much lower than that of conventional Si power diode when the operating current densities do not exceed 1000 A/cm^2, which is very good for getting lower operating loss. The forward voltage drop of the Si diode is 0.66 V whereas that of the SJ SiGe diode is only 0.52 V at operating current density of 10 A/cm^2. The breakdown voltages are 203 V for the former and 235 V for the latter. Compared with the conventional Si power diode, the reverse recovery time of SJ SiGe diode with 20 per cent Ge content is shortened by above a half and the peak reverse current is reduced by over 15%. The SJ SiGe diode can remarkably improve the characteristics of power diode by combining the merits of both SJ structure and SiGe material.

Keywords: super junction, SiGe diode, fast switching, low-loss
PACC: 7340L, 7360P

1. Introduction

The power semiconductor industry has grown steadily in the past decade from $2.7 billion in 1992 to over $11 billion in 2001 due to the rapid proliferation of power electronics in many fields like telecommunications, computers, consumer, transportation, utilities, industrial and other energy conversion applications.[1] The increasing application requires power devices to have higher performance. Therefore, improving the trade-off between the breakdown voltage, forward voltage drop and switching time should be importantly taken into consideration in the power device design.

For the widely used power diode at present, the performance of state-of-the-art Si p-i-n diode is now approaching the theoretical limits.[2] Currently available alternatives to Si p-i-n diodes all have their disadvantages. Although the performance of silicon carbon (SiC) power diodes is demonstrated to be superior to Si diodes,[3−6] the use of wide-band gap materials is cost-prohibitive and they cannot be integrated with the silicon process. With the widespread use of silicon germanium (SiGe) material, the shallow SiGe/Si hetero-junction becomes an important constituent. The SiGe power devices have been gradually assuming great importance[7−11] and we have done much work on the reach of SiGe fast switching power diodes.[12−14] Recently, a new device concept called the super junction (SJ) device is gaining more and more attention.[15−20] This concept pushes the power MOSFETs utility in higher breakdown voltage (BV) and high wattage (lower on state resistance R_{on}) applications by breaking the so-called silicon limit ($R_{on} = BV^{2.5}$).[21] By combining the merits of both SJ structure and SiGe material, a novel SJ SiGe power diode which has a columnar structure of alternating p^- and n^- doped pillar in the base region and has far thinner strained SiGe p^+ layer is proposed. The SJ SiGe diode shares many similarities with the SJ MOSFET.

2. Device structure

The schematic cross-section of the conventional SiGe diode is shown in Fig.1(b), which is analogous

*Project supported by the National Natural Science Foundation of China (Grant No 50477012), the Doctoral Program Foundation of Institutes of Higher Education of China (Grant No 20050700006) and the Special Scientific Research Program of the Education Bureau of Shaanxi Province, China (Grant No 05JK268).

†E-mail: mali@xaut.edu.cn

with that of conventional Si $p^+n^-n^+$ diode (Fig.1(a)) except that the former diode has far thinner strained SiGe p^+ region whose thickness is about 20–50 nm. Compared with the conventional SiGe diode, the n^- base region of SJ SiGe diode is substituted by a columnar structure of alternating p^- and n^- doped pillars (as shown in Fig.1(c)). These pillars extend across the n^- base region from anode to cathode. The height of these pillars coincides with the thickness of the n^- base region. In a SJ power device, widths and doping concentrations of both pillars are usually designed to have exactly the same values and can be changed with the requirement of sustaining the reverse blocking voltage.

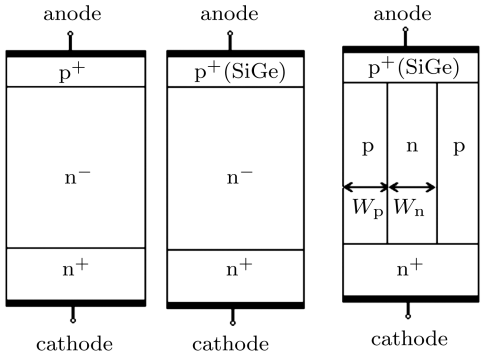


Fig.1. The schematic cross-section of Si $p^+n^-n^+$ diode (a), conventional SiGe diode (b) and SJ SiGe diode (c).

In the following, we present numerical simulation results obtained with the MEDICI software release 4.1.[22] In order to achieve realistic results, several important material parameters used in MEDICI such as energy bandgap and mobility are adjusted to obtain the closest agreement with the published material data of SiGe. SJ power structures present a challenge with respect to numerical grid generation: a large portion of the n^- base of conventional power devices can be represented by using comparatively coarse grids in both x- and y-directions. The SJ of a SJ structure requires narrow grids in the vertical (from cathode to anode) as well as in the horizontal (perpendicular to the SJ) directions. A numerically feasible grid for a SJ SiGe diode may have ten times the number of grid points as a comparable Si $p^+n^-n^+$ diode grid. In this paper, all diodes are assumed to have the same base region thickness of 10 μm so as to compare conveniently, homogeneous doping concentration in both p^- and n^- doped pillars of SJ diodes is at 1×10^{15} cm^{-3} and both pillars have a width of 6 μm. The thickness of strained SiGe p^+ region is 50 nm and the Ge content is 20%.

Conventional SiGe diodes are formed by epitaxial growth on Si crystal substrate. First a thick ($\sim$10 μm) n^- silicon layer is grown. It is sufficient to support the required reverse breakdown voltage. Then, a thin ($\sim$50 nm) strained SiGe layers, as a heavily doped p^+ region, is grown. The SJ structure can be implemented with only one additional mask. Lateral diffusion of p-pillar in the n^- base region can be controlled precisely by boron implantation.

3. Results and analysis

Figure 2 shows the comparison of the forward conduction characteristics among Si $p^+n^-n^+$ diode, SiGe diode and SJ SiGe diode.

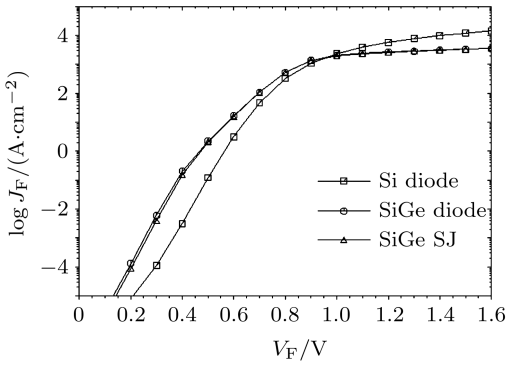


Fig.2. Forward conduction characteristics comparison of Si $p^+n^-n^+$ diode, SiGe diode and SJ SiGe diode.

It can be seen that the forward voltage drop of SiGe diode and SJ SiGe diode is much lower than that of Si $p^+n^-n^+$ diode when the operating current densities do not exceed 1000 A/cm^2, which is very good for getting lower operating loss. The forward voltage drop of the former two diodes is only 0.52 V whereas that of Si diode is 0.66 V at operating current density of 10 A/cm^2. For p^+(SiGe)/n^-(Si) hetero-junction, there are discontinuities in the conduction band (ΔE_c) and valance band (ΔE_v), but the majority of discontinuities occur in valence bands (Fig.3), it will produce an additional barrier for holes diffusing from p^+ (SiGe) layer to n^- region.

Therefore the current density of SiGe power diodes is determined by the diffusion current of electrons in the p^+(SiGe) layer and the hole current can be ignored. The SJ SiGe diode doping profile and the corresponding injected charge distribution with the forward current density in the p^- doped pillar is

provided in Fig.4. With the increase of current density, the injected carrier density also increases and ultimately exceeds the relatively low background doping of p^- doped pillar.

The blocking capability is effectively improved for SJ SiGe diode, as illustrated in Fig.5. Compared with conventional SiGe diode and Si $p^+n^-n^+$ diode, the SJ SiGe diode can obtain higher blocking voltage. As shown in Fig.5, the blocking voltage of SJ diode is 235.5V whereas that of the other two diodes is only 203.5 V. Due to introducing the columnar structure of alternating p^- and n^- doped pillar in the n^- base region, there is a lateral depleted SJ region and perfect compensation of the charges in the pillars which results in higher blocking voltage. That is, the SJ diode thickness required for a given blocking voltage is smaller than that of conventional Si and SiGe diodes which is very good for getting lower forward voltage drop and faster switching speed.

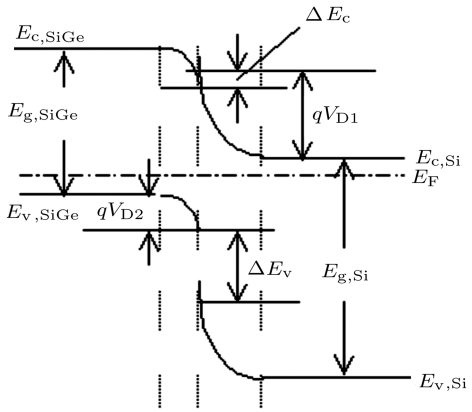


Fig.3. The equilibrium band diagram of p^+(SiGe)–n^-(Si) hetero-junction.

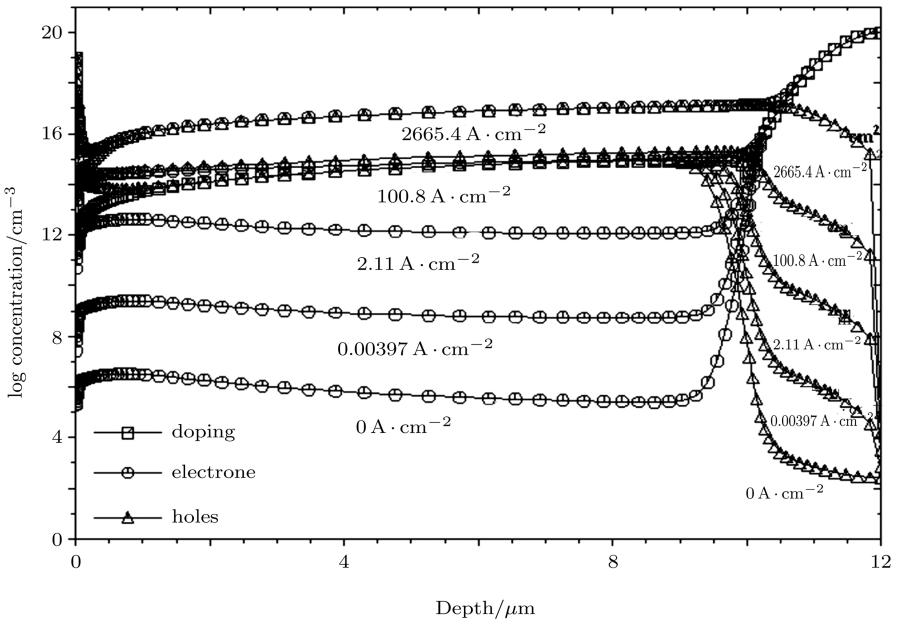


Fig.4. SJ SiGe diode doping profile and the corresponding injected charge distribution with the forward current density.

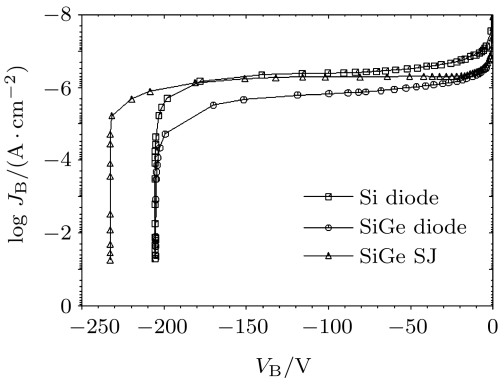


Fig.5. Reverse blocking characteristics comparison of Si $p^+n^-n^+$ diode, SiGe diode and SJ SiGe diode.

The electric field profile is almost flat throughout the SJ region. This is in contrast to the triangular or trapezoidal shape of the electric field in blocking punch and non-punch through conventional diode. Figure 6 shows distributions of electric field lines in a SJ SiGe diode and a conventional Si diode. The reverse breakdown voltage V_{BR} of the SJ diode can be approximately expressed as $V_{BR} = E_c d$, where E_c is the critical breakdown electric field and d is the depth of pillars.

Figure 7 shows the doping profile (C_d) and electron, hole density distributions (C_e, C_h) in n pillar

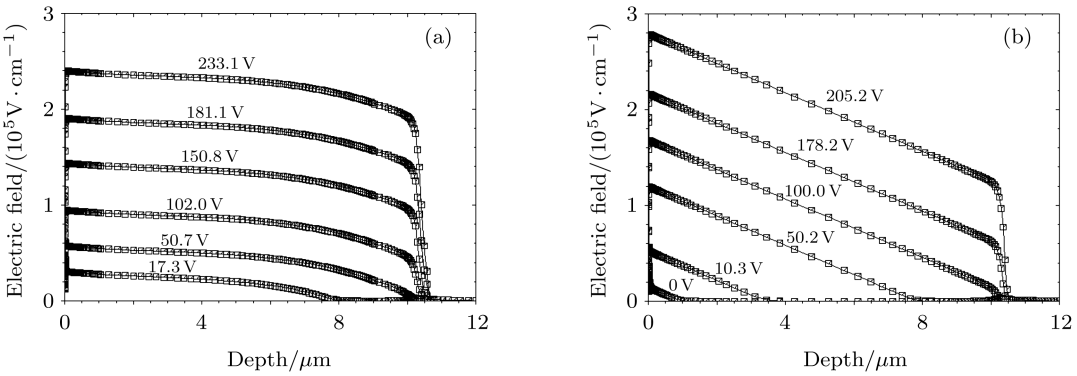


Fig.6. Distributions of electric field lines in a blocking SJ SiGe diode (a) and Si $p^+n^-n^+$ diode (b).

of SJ SiGe diode during reverse block period at different reverse-bias voltage. It can be seen that the carriers in n pillar are depleted primarily on the n^+-side and the depletion region quickly expands toward p^+-side. When the device is broken down, both carrier density increases abruptly and ultimately exceeds the low background doping concentration (Fig.7(d)).

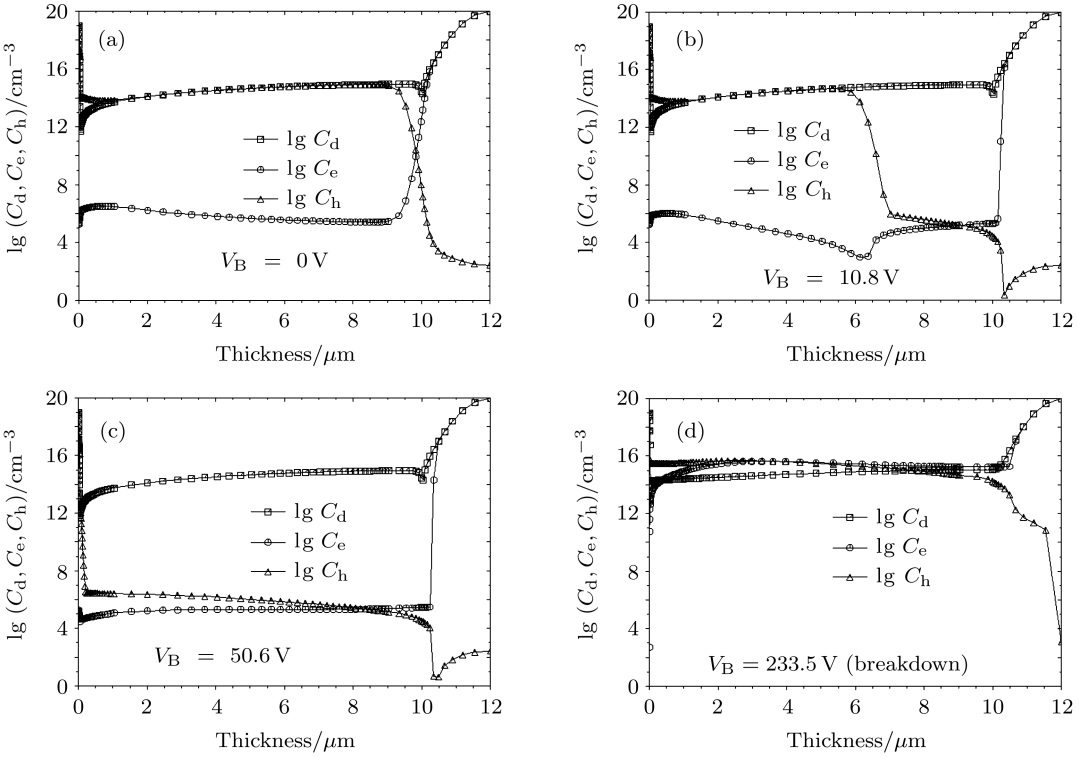


Fig.7. Doping profile(C_d) and electron, hole density distributions (C_e, C_h) in n pillar of SJ SiGe diode during reverse block period at 0 V(a), 10.8 V(b), 50.6 V(c) and 233.5 V(breakdown) (d).

The test circuit for a diode from forward to reversed bias is shown in Fig.8.

These carriers injected from the anode and cathode regions during forward conduction must be removed from the base region to sustain the reverse blocking voltage. The removal of the carriers occurs by both the flow of reverse current out of the anode prior to the establishment of a junction depletion layer and by the recombination of the free carriers. Using charge control analysis

$$\frac{\mathrm{d}Q(t)}{\mathrm{d}t} = J(t) - \frac{Q(t)}{\tau_{\mathrm{HL}}}, \tag{1}$$

where $Q(t)$ is the stored charge per unit area in the

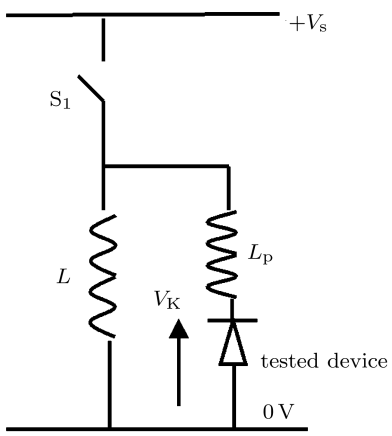


Fig.8. Circuit used to emulate diode switching.

power diode due to on-state current flow, τ_{HL} is the high-level lifetime. The reverse recovery time t_{rr} is determined by relating the charge removed during the reverse recovery process to the initial stored charge with the middle region. It can be obtained as follows:

$$\frac{1}{2}J_{PR}t_{rr} = Q_s = qn^*2d = J_F\tau_{HL}, \quad (2)$$

$$t_{rr} = 2\tau_{HL}\frac{J_F}{J_{PR}}, \quad (3)$$

where J_{PR} is the peak reverse recovery current density, Q_s the initial stored charge, n^* is the average carrier concentration in the base region, d is the half thickness of base region, J_F is the operating current density. For p^+ (SiGe)/n^-(Si) hetero-junction, the majority of band discontinuities occur in valence bands ($\Delta E_c \ll \Delta E_v$) (Fig.3), it will produce an additional barrier for holes diffusing from p^+ (SiGe) layer to n^- region. Therefore, there is less stored charge Q_s for the SiGe diodes than the Si diodes at the given forward current density, which is very good for gaining shorter reverse recovery time.

In addition, owing to the columnar structure of alternating p^- and n^- doped pillar in the base region of SJ SiGe diode, the recombination process of carriers becomes acute which results in shorter reverse recovery time (Figs.9 and 10). Also it can be seen that the peak reverse current is decreased which is very useful for the fast switch diode. Compared with conventional Si diode, the reverse recovery time of SJ SiGe diode with 20 per cent Ge content is shortened by above a half and the peak reverse current are reduced by over 15%. However, the soft recovery characteristics are degenerated for the SJ SiGe diode at the same time of getting shorter recovery time. We can add bottom assist layer in the base region of the SJ constituting the so called semi-super junction[23−25] to improve the soft recovery characteristics.

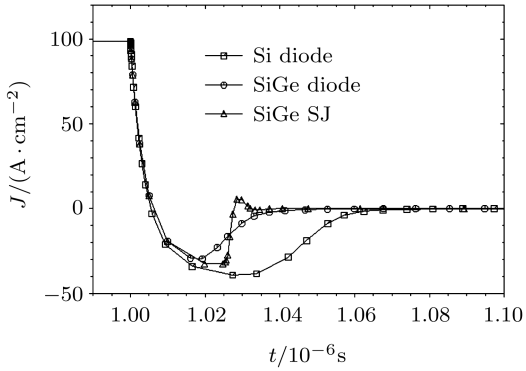


Fig.9. Comparison of reverse recovery currents characteristics among Si $p^+n^-n^+$ diode, SiGe diode and SJ SiGe diode.

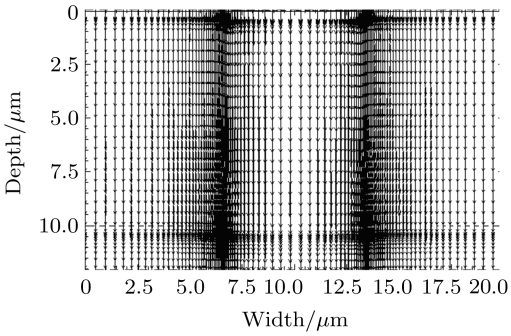


Fig.10. The current vectors in a SJ SiGe diode for the transition from forward bias to reverse bias.

4. Conclusions

The novel SJ SiGe power diode can improve notably characteristics of the power diode by combining both merits of SJ structure and SiGe material. The SJ structure is introduced by the columnar structure of alternating p^- and n^- doped pillar in the base region. Compared with conventional Si $p^+n^-n^+$ diode, the forward voltage drop of SJ SiGe diode is much lower when the operating current densities do not exceed 1000 A/cm^2, the breakdown voltages is increased by almost 20% and the reverse recovery time of SJ SiGe diode with 20 per cent Ge content is shortened by above a half and the peak reverse current is reduced by over 15%. Thus the SJ SiGe diode can be operated at high-power fast switching and low losses applications especially in power integrated circuits.

References

[1] Bauer F D 2004 *Solid-State Electronics* **48** 705

[2] Deboy G, Marz N, Stengl J P, Strack H, Tihanyi J and Weber H 1998 In: *Proc. IEDM* (San Francisco) p683

[3] Shenai K, Trivedi M and Neudeck P G 2002 *IEEE Trans. Electron Devices* **49** 1648

[4] Wahab Q 1998 *Appl. Phys. Lett.* **72** 445

[5] Dyakonova N V, Ivanov P A, Kozlov V A, Levinshtein M E, Palmour J W, Rumyantsev S L and Singh R 1999 *IEEE Trans. Electron Devices* **46** 2188

[6] Zhang F and Li C F 2004 *Chin. Phys. Lett.* **21** 2305

[7] Vashaee D and Shakouri A 2007 *Semicond. Sci. Technol.* **22** S84

[8] Hung C C, Liao W S, Huang S Y, Chen K M, Huang G W and Lien C H 2008 *Jap. J. Appl. Phys.* **47** 2872

[9] Vashaee D and Shakouri A 2007 *J. Appl. Phys.* **101** 034502

[10] Keerti A and Pham A V H 2007 *IEEE Trans. Microwave Theory and Techniques* **55** 207

[11] Brown A R, Hurkx G A M, Huizing H G A, Peter M S, de Boer W B, van Berkum J G M, Zalm P C, Huang E and Koper N 1998 *IEDM Tech. Dig.* (San Francisco) p699

[12] Gao Y and Ma L 2004 *Chin. Phys. Lett.* **21** 414

[13] Ma L Gao and Y Wang C L 2004 *Chin. Phys.* **13** 1114

[14] Qi H and Gao Y 2003 *Proc. APEC* (Miami: Courtesy Associates) p964

[15] Zhang B, Chen L, Wu J and Li Z J 2005 *Proc. ICCCAS* China, Hong Kong p1402

[16] Miura M, Nakamura S, Suda J, Kimoto T and Matsunami H 2003 *IEEE Electron Device Lett.* **24** 321

[17] Henson T and Cao J 2003 *Proc. ISPSD* (Cambridge, UK) p37

[18] Chen X B and Sin J K O 2001 *IEEE Trans. Electron Devices* **48** 344

[19] Cortés I, Fernández M P, Flores D, Hidalgo S and Rebollo J 2008 *Semicond. Sci. Technol.* **23** 9

[20] Chen W, Zhang B and Li Z J 2007 *Semicond. Sci. Technol.* **22** 464

[21] Chen X B, Mawby P A and Board K 1998 *Microelectron. J.* **29** 1005

[22] Medici 4.1User's manual 2001 (Fremont: Avanti Corporation)

[23] Saito W, Omura I, Aida S, Koduki S, Izumisawa M, Yoshioka H and Ogura T 2005 *Proc ISPSD* (Santa Barbara, CA) p27

[24] Cheng J B, Zhang B, Duan B X and Li Z J 2008 *Chin. Phys. Lett.* **25** 262

[25] Duan B X, Zhang B and Li Z J 2007 *Chin. Phys.* **16** 3755